Journal of Materials Chemistry

Cite this: J. Mater. Chem., 2012, 22, 9939

www.rsc.org/materials

PAPER

Tunable reinforcement of epoxy-silica nanocomposites with ionic liquids†

Ricardo K. Donato,[ab] Katarzyna Z. Donato,[a] Henri S. Schrekker[b] and Libor Matějka*[a]

Received 10th February 2012, Accepted 19th March 2012
DOI: 10.1039/c2jm30830d

Imidazolium ionic liquids (ILs) have the capacity to exert multiple functions as additives for the formation of epoxy-silica nanocomposites, *via* the simultaneous sol–gel process and epoxy network build-up. This study addresses the effect of ILs on the reinforcement of tensile properties in rubbery epoxy-silica nanocomposites, allowing property tailoring. The use of ILs together with the coupling agent 3-glycidyloxypropyltrimethoxysilane (GTMS) created a synergic action between physical and chemical interfacial bonding, enabling an increase in toughness without a considerable loss of stiffness. The best tensile property balance was obtained with IL 1-triethylene glycol monomethyl ether-3-methylimidazolium methanesulfonate and GTMS. The rubbery nanocomposite produced was remarkably both stiffer and tougher than the unmodified epoxy-silica system, displaying *ca.* 6 times higher modulus and tensile strength as well as more than 10 times higher energy to break.

Introduction

Systems with tailored properties are highlighted in modern materials chemistry. The ability to significantly change polymer properties through small modifications of various parameters is the ideal to be reached. Within this perspective, polymer nanocomposites are advanced materials that meet this requirement. The application of silica nanofillers formed *in situ* by the sol–gel process is a feasible option, where the properties of the silica-containing polymer nanocomposites are mainly governed by the silica structure and the nanocomposite morphology. This process, involving the hydrolysis and polycondensation of alkoxysilane precursors, allows the silica structure control based on the adjustment of reaction conditions, like, for instance: type of catalyst (acidic, basic or nucleophilic), water content, type of solvent and the use of a template. Recently, the application of ionic liquids (ILs) was shown to be a promising strategy for nanocomposite structure control.[1–4] The ILs also affect the mechanical and thermal properties of polymer nanocomposites by serving as surfactants and improving the dispersion of nanofillers, such as graphene, clay or carbon nanotubes (CNTs), in a polymer matrix. Applications of ILs in polymer electrolyte membranes using protic ionic liquids and graphene;[5] in polyethylene-clay nanocomposites as a clay modifier instead of quaternary ammonium salts;[6] and as a dispersant for CNTs in polymer matrices, both using ILs-CNT "bucky gel"[7] or ILs covalently attached to the polymer backbone *via* "click chemistry",[8] are only a few of the examples.

ILs are organic salts that are in the liquid state at temperatures of 100 °C or below. They present ionic–covalent crystalline structures and differentiated properties such as: insignificant flammability and volatility, high thermal and chemical stability, wide electrochemical windows, good thermal conductivity, and high ionic mobility and stability in the presence of air and moisture.[9–12] Furthermore, ILs can be used as "molecular templates" in the sol–gel silica process due to their special molecular arrangements. The ILs' self-organization and selective interaction with substrates and growing particles, provoking their pre-organization, enables silica structure control.[1,4,13]

Recently, we have prepared epoxy-silica nanocomposites in the presence of ILs as multifunctional agents to control their structure, morphology and thermomechanical properties.[4] The silica phase was formed *in situ* within the simultaneously built epoxy network by the sol–gel process from tetraethoxysilane (TEOS). Various methylimidazolium based ILs have been shown to serve as catalysts for the sol–gel process, as silica morphology controllers and as surfactants or templates controlling the silica–epoxy interactions. The IL 1-triethylene glycol monomethyl ether-3-methylimidazolium methanesulfonate (C_7O_3MImMeS) acts as an acidic catalyst, promoting fine nanocomposite morphology with well dispersed silica nanodomains. This IL promoted reinforcement of the nanocomposite, *i.e.* an increase in the rubbery modulus. The best hybrid system homogenization, however, was achieved by using IL 1-*n*-decyl-3-methylimidazolium tetrafluoroborate (C_{10}MImBF_4) in the presence of HCl. This nanocomposite showed the most significant modulus enhancement due to physical crosslinking by the ordered domains of the IL decyl-substituents.[4]

[a]*Institute of Macromolecular Chemistry, Academy of Sciences of the Czech Republic, Heyrovský Sq. 2, 162 06 Prague 6, Czech Republic. E-mail: matejka@imc.cas.cz; Fax: +420 296809410*
[b]*Laboratory of Technological Processes and Catalysis, Institute of Chemistry, Universidade Federal do Rio Grande do Sul, Av. Bento Gonçalves 9500, Porto Alegre-RS, Brazil*
† Electronic supplementary information (ESI) available. See DOI: 10.1039/c2jm30830d

Preliminary results have proven also an effect of ILs on the enhancement of ultimate tensile properties, including the toughness of the rubbery epoxy nanocomposites. The reinforcement of elastomers by *in situ* formed silica and their tensile properties were described by Mark[14] and Bokobza.[15] The *in situ* generation of silica in the poly(dimethylsiloxane) networks and in natural rubber resulted in organic–inorganic hybrids with increased modulus and tensile strength as well as a high finite extensibility. Generally, rubber reinforcement is defined as a simultaneous increase in stiffness (modulus), tensile strength, finite extensibility and toughness. The modulus enhancement is given by (a) the hydrodynamic effect of hard filler particles in a soft matrix,[16] which refers to strain amplification (internal local strain is higher than the external one) due to the presence of inextensible particles and by (b) interphase filler–matrix interactions leading to the immobilization of the interfacial polymer layer, thus increasing the effective filler volume.[17,18] The modulus increase by hard fillers, however, is often accompanied by a decrease in the material extensibility and toughness. Hence, the challenge of this approach consists in the optimization of the balance between stiffness, strength and toughness.

In the case of composites, the morphology involving size of the inorganic filler phase and homogeneity of its dispersion in a matrix is of high importance. Moreover, the organic–inorganic interface plays a crucial role. The modification of a nanofiller surface to improve its dispersion and strengthen the interphase interactions results in the enhancement of the nanocomposite's mechanical properties. Coupling agents, such as 3-glycidyloxypropyltrimethoxysilane (GTMS) or aminopropyltrimethoxysilane are often used to increase the interaction in epoxy-silica nanocomposites, leading to system homogenization and improved mechanical properties, mainly in glassy epoxy thermosets.[19,20]

In this paper we have studied the effect of ILs and GTMS on the tensile properties (Young's rubbery modulus (E), tensile strength (σ_b), elongation at break (ε_b), *i.e.* material extensibility, and toughness) of epoxy-silica nanocomposites. The rubbery epoxy network DGEBA-poly(oxypropylene)diamine (Jeffamine D2000) was reinforced with silica formed *in situ* from TEOS and GTMS, used as a coupling agent to strengthen the interface interaction. Within this context, the novelty of this paper consists in applying ILs to enhance and balance the tensile properties of the corresponding elastomer nanocomposites. The ILs $C_7O_3MImMeS$ and $C_{10}MImBF_4$ as well as 1-*n*-hexyl-3-methylimidazolium methanesulfonate ($C_6MImMeS$) were applied as multifunctional agents.

The unique and efficient way of morphology and interface interaction control by ILs and GTMS afforded nanocomposites with remarkably enhanced tensile mechanical properties. As a result, the nanocomposites involving an optimal GTMS content showed well-balanced tensile behavior, including a significant increase in both modulus and toughness.

Experimental

Materials

Organic system components. The epoxy network was prepared by curing the diglycidyl ether of bisphenol A (DGEBA) based resin, Epilox A 19-03 (Leuna–Harze GmbH) with poly(oxypropylene)diamine, Jeffamine® D2000 (M = 1970) (Huntsman Inc.). The equivalent weights of the epoxy group in DGEBA and the NH group in Jeffamine® D2000 were, respectively, E_E = 187 g mol^{-1} epoxy groups and E_{NH} = 492 g mol^{-1} NH groups.

Inorganic system components. Tetraethoxysilane (TEOS) and 3-glycidyloxypropyltrimethoxysilane (GTMS) were used as received (Fluka).

IL synthesis

Three ILs were synthesized through halide-free methodologies, as described in the literature:[21,22] $C_{10}MImBF_4$, $C_7O_3MImMeS$ and $C_6MImMeS$ (Fig. 1). The purity of the synthesized ILs was checked by ^{1}H- and ^{13}C-NMR (see supplementary information†).

Synthesis of the epoxy-silica nanocomposites

The nanocomposites were prepared from a stoichiometric mixture of the organic components, DGEBA and D2000 (the ratio of functionalities $C_{NH} : C_{epoxy} = 1 : 1$) and the inorganic phase components, TEOS, GTMS and H_2O. HCl and/or IL were used as the catalyst/additive where indicated. The hybrids were synthesized at the ratios of functionalities DGEBA : D2000 : TEOS = 1 : 1 : 6 (TEOS is a tetrafunctional reagent with respect to the sol–gel process). This composition corresponds to ~11 wt% of silica (*i.e.* around 5 vol%) according to the TGA analysis.

The hybrids modified with the coupling agent GTMS were prepared by substituting a fraction of DGEBA by GTMS while keeping the epoxy groups' concentration constant and the total ratio of functionalities stoichiometric. The content of GTMS (x) in the nanocomposite synthesis was characterized by the fraction of epoxy groups of DGEBA replaced by GTMS:

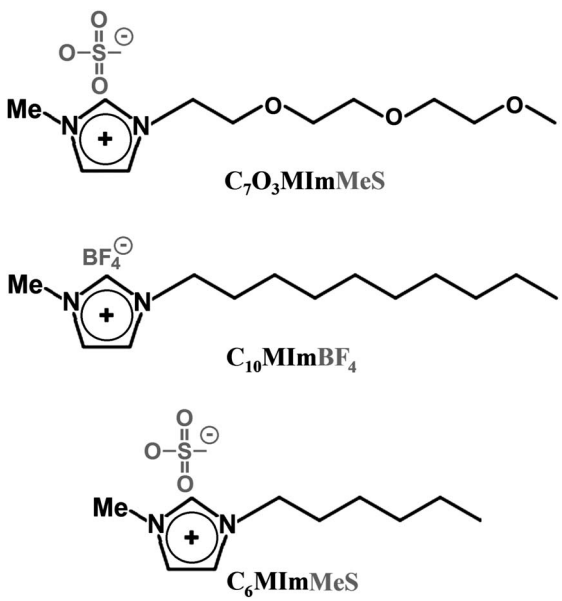

Fig. 1 Structure of the ILs prepared and studied in this work.

x = epoxy (GTMS)/[epoxy (DGEBA) + epoxy (GTMS)] (1)

The composition of the nanocomposites involving 10–60 mol % of epoxy groups from GTMS: $x = 0.10$–0.60, corresponds to 0.5–3.0 wt% of silsesquioxane structures under a complete GTMS hydrolytic condensation.

Two synthetic procedures were employed.[18,23,24]

One-step procedure. The reaction components, both organic and inorganic, were mixed and reacted. The system was kept for 2 h at 60 °C, heated to 130 °C for 2 days and post-cured and dried under vacuum at 150 °C for 2 h.

Two-step procedure with pre-hydrolyzed TEOS. The different applied approaches of this synthetic strategy are demonstrated in Scheme 1. (1) TEOS was pre-hydrolyzed in the presence of HCl (reaction 1a) and/or IL (reaction 2a) at room temperature for 1 h. (2) The pre-hydrolyzed TEOS with (reaction 2b) or without ILs (reaction 1b) was mixed with the organic phase components DGEBA and D2000 and the subsequent curing procedure was the same as in the case of the one-stage process.

The systems were mechanically stirred during the whole synthesis process, up to the curing stage when they were transferred to a Teflon wafer mold and cured to form 2 mm thick

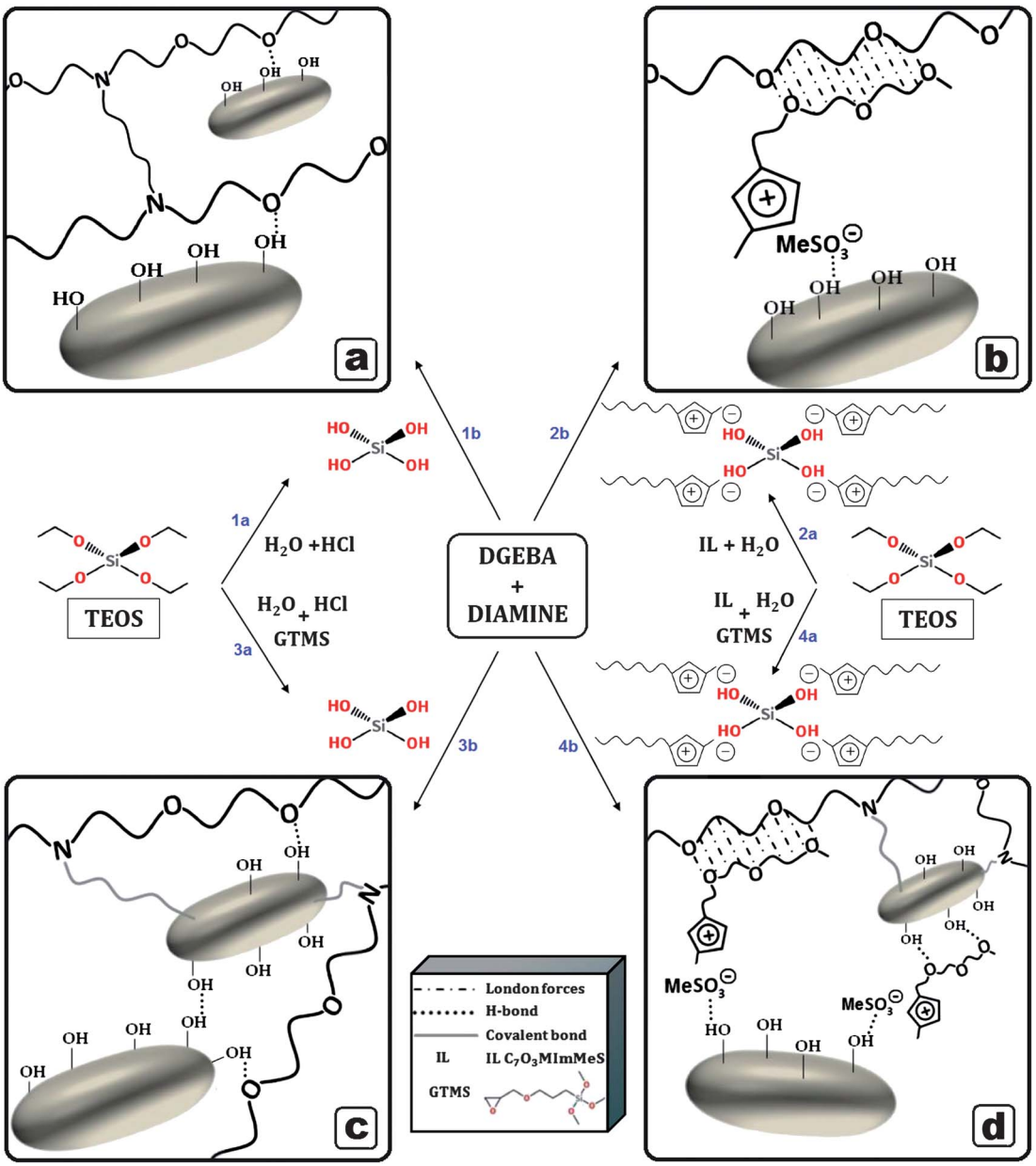

Scheme 1 Applied synthetic approaches for the preparation of epoxy-silica nanocomposites and generalized representation of the corresponding network interphase interactions: (a) systems without and (b) with IL $C_7O_3MImMeS$, and (c) with GTMS in the absence and (d) presence of IL $C_7O_3MImMeS$.

samples. Both nanocomposites prepared in the one-step and two-step procedures without the addition of ILs were used as the references.

Two-step procedure with pre-hydrolyzed TEOS and GTMS. TEOS and GTMS were mixed and subjected to the same procedure as the two-step process without GTMS, with (reactions 4a and 4b) or without IL (reactions 3a and 3b).

The ILs were applied only in the two-step procedure, with and without GTMS, and the final system contained ~0.6 wt% of IL.

Due to the broad range of variables applied in the synthesis of the hybrids, a sample codification was used where necessary. The neat epoxy is referred to as **a**; the one-step and two-step process hybrids without IL as **b** and **c**, respectively; the two-step process in the presence of the ILs $C_7O_3MImMeS$, $C_{10}MImBF_4$ and $C_6MImMeS$ as **d**, **e** and **f**, respectively; the number following the sample code refers to the applied GTMS percentage and the asterisk (*) is used for samples without application of TEOS; *e.g.*, sample **d60*** refers to the nanocomposite prepared by the two-step process in the presence of IL $C_7O_3MImMeS$, addition of 60% of GTMS and with no TEOS applied.

Methods

Small-angle X-ray scattering (SAXS). The experiments were performed using a pinhole camera (Molecular Metrology SAXS System) attached to a microfocused X-ray beam generator (Osmic MicroMax 002) operating at 45 kV and 0.66 mA (30 W). The camera was equipped with a multiwire, gas-filled area detector with an active area diameter of 20 cm (Gabriel design). Two experimental setups were used to cover the q range of 0.004–1.1 $Å^{-1}$, where $q = (4\pi/\lambda)\sin\theta$ (λ is the wavelength and 2θ is the scattering angle). The scattering intensities were placed on an absolute scale using a glassy carbon standard. The nanocomposites were measured as thin films.

Dynamic mechanical analysis (DMA). A Rheometer ARES (Rheometric Scientific) was used to follow the dynamic mechanical behavior of the networks. The temperature dependence of the complex shear modulus of rectangular samples was measured by oscillatory shear deformation at a frequency of 1 Hz and a heating rate 2 °C min^{-1}.

Tensile tests. Tensile tests were carried out at 22 °C using an Instron 5800 apparatus at a crosshead speed of 1 mm min^{-1}. At least five dumb-bell shaped specimens were tested for each sample. The Young's modulus, E, the stress to break, σ_b, and elongation to break, ε_b, were evaluated. In addition, the energy to break obtained from the area under the stress–strain curve was determined as a standard measure of the elastomer toughness.

For the Mullins-type experiments a set of extension–retraction cycles was carried out. After each cycle the specimen was kept at rest for ~15–30 min to reach a quasi-equilibrium state. The tension set, however, was not removed before the subsequent extension.

Results and discussion

The tensile properties of the epoxy-silica elastomer nanocomposites strongly depend on the system morphology and interfacial interactions. Therefore, a key point to enhance the mechanical properties consists of the control of the structure and morphology. As it was previously determined, such control can be achieved by the nanocomposite synthesis procedure,[23,24] applying either the GTMS coupling agent[19,20] or ILs.[4]

Formation and morphology of epoxy-silica nanocomposites

The epoxy-silica nanocomposites were prepared by the simultaneous build-up of the rubbery epoxy-amine network DGEBA-D2000 and the silica phase formation from TEOS using the sol–gel process. The incorporation of *in situ* produced silica leads to the reinforcement of the epoxy network with dependence on the resulting nanocomposite morphology determined by the sol–gel reaction conditions.[18,25] The one-step polymerization leads to a relatively heterogeneous system with large silica domains (~100–300 nm in diameter) dispersed in the matrix. On the contrary, a fine nanostructured silica morphology (~50–100 nm) is formed under the two-step polymerization due to a stronger epoxy-silica interphase interaction that improves the system compatibility.[4,24] This is a result of acid catalysis promoting the formation of high silanol (SiOH) contents in the growing and final silica structure. The silanols enable H-bond interactions with the epoxy network involving polyoxypropylene (POP) chains (Scheme 1a).[24,25]

The final structure, morphology and interface interactions of the epoxy-silica nanocomposites were modified and tuned by using ILs and the coupling agent GTMS. Previously, we reported a very fine morphology and a homogeneous silica dispersion in an epoxy matrix achieved by the application of the ILs $C_7O_3MImMeS$ (size of silica domains ~20–50 nm in diameter) and $C_{10}MImBF_4$ in the presence of HCl (size < 10 nm).[4] Scheme 1b shows the effect of $C_7O_3MImMeS$ on the epoxy–silica interface and the compatibilization of the system. Scheme 1c displays the structure of a nanocomposite prepared by using GTMS to form covalent bonding between the silica and epoxy phases. GTMS is incorporated in the epoxy-amine network by the reaction of the glycidyl group with amine, while the methoxy-silane groups undergo hydrolytic condensation to form silsesquioxane (SSQO) domains. The process of GTMS incorporation in the epoxy network is quite complex and depends on the catalysis of the sol–gel reactions. In our case, GTMS was pre-hydrolyzed under acid catalysis in the first step to produce low molecular weight SSQO oligomers with pendant epoxy groups. In the second step (see Experimental section) a fast condensation occurs due to basic catalysis of the reaction mixture by amine D2000, resulting in the formation of polyhedral cage-like poly-SSQO structures with emanating epoxy groups.[26,27] Only then does the slower epoxy–amine reaction becomes operative. The epoxy-amine network is formed and the epoxy functionalized SSQO clusters are covalently bound to the network.[28] Co-condensation of the SSQO structures with the silica domains formed from TEOS results in a better nanosilica dispersion. The SAXS profiles in Fig. 2 show homogenization of the epoxy-silica nanocomposite by using GTMS. The profiles of the silica or

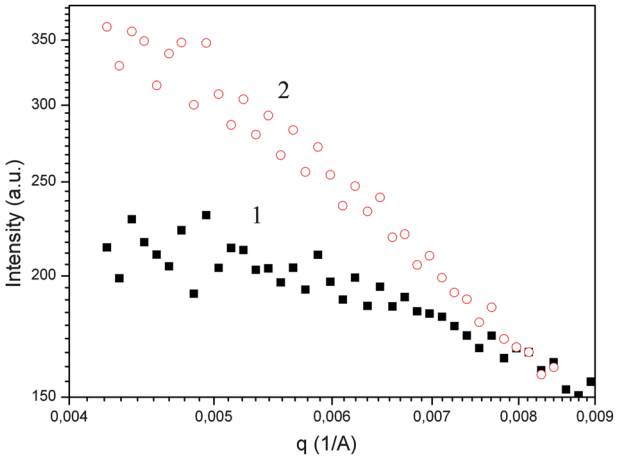

Fig. 2 SAXS diffractograms of epoxy-silica nanocomposites with IL $C_7O_3MImMeS$: (1) with and (2) without GTMS.

silica/SSQO clusters belong to the systems formed in the presence of IL $C_7O_3MImMeS$ with and without the addition of 20% GTMS. The levelling off of the intensity curve at low scattering angles in the GTMS containing nanocomposite proves the presence of smaller scattering objects (silica/SSQO domains). This system's interphase interactions are demonstrated in Scheme 1d.

Tensile properties

Table 1 and Fig. 3 summarize and represent the tensile properties of all studied epoxy materials. Fig. 4 characterizes the stress–strain tensile behavior dependencies on the synthesis procedure, as well as on the application of GTMS and ILs. The slope of the curves at a low strain is proportional to the modulus and the area under the curve corresponds to the energy to break.

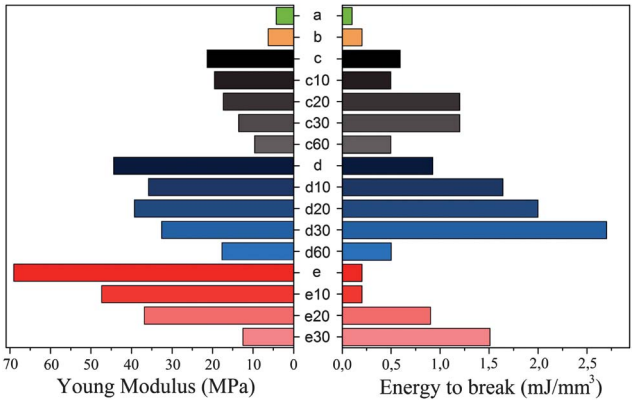

Fig. 3 Tensile property trends: Young's modulus and energy to break of (a) neat epoxy; (b) one-step processed hybrid; (c) two-step processed hybrid with (c10) 10, (c20) 20, (c30) 30 and (c60) 60% of GTMS; (d) hybrid formed by adding IL $C_7O_3MImMeS$ with (d10) 10, (d20) 20, (d30) 30 and (d60) 60% of GTMS; and (e) hybrid formed by adding IL $C_{10}MImBF_4$ with (e10) 10, (e20) 20 and (e30) 30% of GTMS.

The neat epoxy network DGEBA-D2000 showed poor elastomeric tensile properties and a relatively low extensibility (Fig. 4, curve a). The elongation at break reached only 22%. This is a result of a high crosslinking density and short elastically active network chains, $M_C \approx 2000$. The incorporation of an *in situ* formed hard nanosilica phase led to the reinforcement of the rubbery epoxy system (Fig. 4, curve b). The tensile modulus (E) and tensile strength (stress at break) as well as the elongation at break (extensibility) and energy to break, characterizing the material toughness, increased in the one-step formed nanocomposite. The two-step synthesis procedure was more efficient for the tensile property enhancement (Fig. 3 and Fig. 4, curve c) due to the homogeneous formation of smaller silica domains. The system was stiffer but showed a lower extensibility than that

Table 1 Tensile properties of the epoxy-silica/SSQO nanocomposites

Entry	Sample[a]	E/MPa	Tensile strength/MPa	Elongation at break (%)	Energy to break/ mJ mm^{-3}
1	**a**	4.3 ± 0.2	0.8 ± 0.1	22 ± 2	0.10 ± 0.02
2	**b**	6.3 ± 0.3	1.3 ± 0.3	25 ± 5	0.2 ± 0.1
3	**c**	21.9 ± 1.8	4.3 ± 0.4	24 ± 2	0.6 ± 0.1
4	**c10**	19.7 ± 1.3	3.5 ± 0.6	19 ± 3	0.5 ± 0.1
5	**c20**	17.4 ± 1.0	5.1 ± 0.1	42 ± 4	1.2 ± 0.1
6	**c30**	13.6 ± 0.4	5.2 ± 0.6	42 ± 6	1.2 ± 0.3
7	**c60**	9.7 ± 0.1	2.8 ± 0.3	30 ± 3	0.5 ± 0.1
8	**c60***	1.6 ± 0.1	0.4 ± 0.1	33 ± 7	0.09 ± 0.03
9	**d**	44.4 ± 0.8	8.0 ± 0.5	20 ± 1	0.9 ± 0.1
10	**d10**	35.9 ± 1.0	6.6 ± 0.5	35 ± 8	1.6 ± 0.6
11	**d20**	39.3 ± 3.0	8.0 ± 1.0	37 ± 5	2.0 ± 0.4
12	**d30**	32.6 ± 1.0	7.5 ± 0.5	51 ± 9	2.7 ± 0.7
13	**d60**	17.7 ± 0.6	3.7 ± 0.3	24 ± 3	0.5 ± 0.1
14	**d60***	1.4 ± 0.03	0.6 ± 0.1	54 ± 9	0.2 ± 0.1
15	**e**	69.1 ± 11.5	3.7 ± 0.8	7 ± 2	0.2 ± 0.1
16	**e10**	47.4 ± 9.0	3.3 ± 1.6	9 ± 4	0.2 ± 0.1
17	**e20**	36.9 ± 5.5	5.6 ± 1.0	24 ± 3	0.9 ± 0.3
18	**e30**	12.5 ± 0.7	4.2 ± 0.5	53 ± 7	1.5 ± 0.3
19	**f**	37.4 ± 0.8	6.3 ± 0.3	41 ± 6	2.0 ± 0.4

[a] (a) neat epoxy; (b) one-step process hybrid; (c) two-step process hybrid with (c10) 10, (c20) 20, (c30) 30 and (c60) 60% of GTMS; (d) hybrid formed by adding IL $C_7O_3MImMeS$ with (d10) 10, (d20) 20, (d30) 30 and (d60) 60% of GTMS; (e) hybrid formed by adding IL $C_{10}MImBF_4$ with (e10) 10, (e20) 20 and (e30) 30% of GTMS; and (f) hybrid formed adding IL $C_6MImMeS$. The asterisk (*) is used for the samples without application of TEOS.

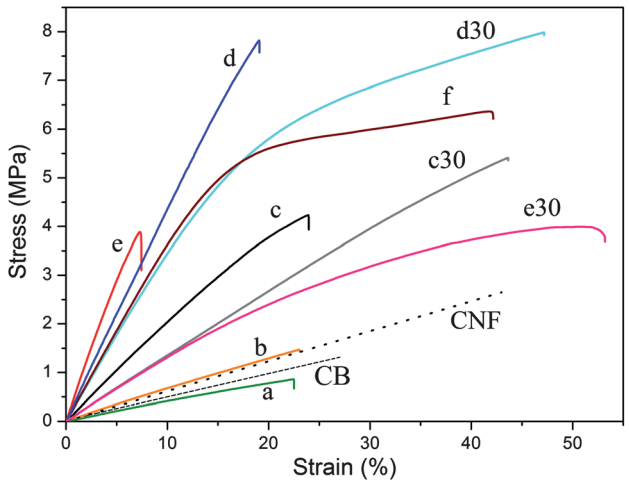

Fig. 4 Stress–strain curves of (a) neat epoxy; (b) one-step processed hybrid; (c) two-step processed hybrid with (c30) 30% of GTMS; (d) hybrid formed by adding IL $C_7O_3MImMeS$ with (d30) 30% of GTMS; (e) hybrid formed by adding IL $C_{10}MImBF_4$ and HCl with (e30) 30% of GTMS; (f) hybrid formed by adding IL $C_6MImMeS$ and comparative literature sample of DGEBA-D2000 reinforced with (CNF) carbon nanofiber.[29]

obtained by the one-step procedure. The modulus and tensile strength increased as a result of a strong silica-epoxy interphase interaction, leading to the immobilization of a fraction of the network chains. This immobilized polymer layer at the interface increases the effective filler content. Moreover, some fraction of the continuous silica phase was formed in the system. Both these effects contributed to the nanocomposite reinforcement but also caused the decrease of the material finite extensibility.[18] The modulus, tensile strength and energy to break increased about 5 times in the two-step nanocomposite in comparison to the neat epoxy network.

The silica reinforcement effect in the rubbery epoxy DGEBA-D2000 nanocomposites can be compared to the effect of carbon black (CB) and carbon nanofibers (CNF), as determined by Chazeau *et al.*[29] The filler loading was somewhat lower (around 3 vol%, compared to ours, ~5 vol%), however, on the other hand, the crosshead speed of the tensile tests was higher (5 mm min^{-1}) with respect to the ones presented in this article (1 mm min^{-1}), leading to a higher measured strength. The carbon based fillers do not interact with the epoxy matrix and the extent of reinforcement is similar to that presented by the one-step synthesis (Fig. 4, curve b *vs.* CB and CNF). While the moduli differ only slightly, the material extensibility increases in the order of the systems; one-step epoxy-silica < epoxy-CB < epoxy-CNF. The "two-step nanocomposite" (curve c), however, showed a remarkably higher stiffness (modulus) and tensile strength then the carbon composites. Furthermore, this nanocomposite displayed similar toughness to the epoxy-CNF system despite a lower extensibility.

Introducing GTMS in the epoxy-silica nanocomposite was found to increase extensibility (Fig. 4, curve c *vs.* c30). The effect of GTMS on the nanocomposite tensile properties was characterized by a decrease in the modulus and an increase in the elongation at break and toughness at low and medium GTMS concentration (Fig. 3). At a high GTMS content, however, all properties were considerably worsened. Very poor tensile behavior was determined in the system containing 60 mol% of epoxy groups from GTMS, $x = 0.60$. Altogether, both the elongation at break and toughness as well as the tensile strength showed a maximum at the optimum 20–30 mol% of GTMS epoxy groups, which corresponds to the substitution of 20–30 mol% of DGEBA epoxy groups with GTMS (1.0–1.5 wt% SSQO domains). The epoxy nanocomposite involving an optimal GTMS amount displayed the same extensibility as the epoxy-CNF system but by a 100% higher modulus, as well as tensile strength and energy to break.

Such tensile behavior results from the competing GTMS effects on the nanocomposite properties. The SSQO nanodomains formed by the sol–gel process serve as nanofillers, reinforcing the organic matrix. Moreover, the coupling agent GTMS improves the system homogeneity and enhances the interfacial interactions (Fig. 2). On the contrary, however, the crosslinking density of the epoxy-amine network is decreased. The epoxy groups issuing from the SSQO clusters, acting as polyhedral network junctions, are closely packed and because of steric reasons both hydrogens from an amino group of the D2000 diamine react with the epoxy groups from the same cluster. Due to this intramolecular reaction the tetrafunctional diamine becomes bifunctional.[30] Moreover, part of the sterically hindered epoxy groups remain unreacted as determined by Macan *et al.*[31] As a result, the network crosslinking density is diminished and the modulus decreases. Replacing the rigid DGEBA with GTMS produces the SSQO domains with dangling flexible glycidyloxypropyl substituents thus turning the system less stiff and more ductile.

The weight fraction of SSQO domains in the nanocomposites was relatively low (0.5–3.0 wt%) compared to the TEOS nanosilica amount (~11 wt%). Therefore, the reinforcing effect of the SSQO nanostructures was not as important with respect to the nanosilica filler formed from TEOS. This was evidenced by the fact that the tensile properties of the nanocomposites prepared in the absence of TEOS were dramatically worse. The modulus in the hybrids with the highest GTMS amount, $x = 0.60$, decreased 6 and 13 times, respectively, in the absence of TEOS (Table 1, entries 7 *vs.* 8 and 13 *vs.* 14).

Consequently, the main GTMS effect consisted of the hybrid homogenization and modification of the epoxy network structure, making it more flexible and less stiff. An increase in both the elongation at break and the energy to break by approximately 2 times was determined for the nanocomposites containing 20–30 mol% GTMS, compared to the two-step processed epoxy-silica hybrid (Fig. 4 and Table 1, entry 3 *vs.* 5 and 6). At the same time, however, the modulus was significantly lowered. Such a loss of the nanocomposite stiffness can be compensated by ILs showing a considerable stiffening effect. Previously, it was proven that ILs $C_7O_3MImMeS$ (with or without HCl) and $C_{10}MImBF_4$ (with HCl) strongly enhance the modulus of epoxy-silica nanocomposites.[4] A low IL content of just ~0.5 wt% was sufficient for increasing the shear modulus by an order of magnitude.

Fig. 4 illustrates the high initial slopes of the stress–strain curves of the $C_7O_3MImMeS$ (curve d), $C_{10}MImBF_4$ (curve e) and $C_6MImMeS$ (curve f) containing systems. The application of IL $C_{10}MImBF_4$, in a synergic action with HCl (two-step process), led to the most stiff but brittle material. The tensile modulus E of

the nanocomposite increased by more than 200% with respect to the hybrid prepared without IL by the two-step process (Table 1, entry 15 *vs.* 3). However, the material exhibited a small elongation at break and low toughness. In our previous paper we proposed that the high modulus could be the result of physical crosslinking due to self-assembly of the IL C_{10}-chains.[4] The low extensibility of the system is a consequence of the very high crosslinking density. Very promising and better balanced tensile properties were achieved by using IL C_7O_3MImMeS. The corresponding nanocomposite displayed an enhancement of the modulus (~100%), strength (~100%) and energy to break (~50%) when compared to the best previously obtained IL free system (two-step). Due to the IL promoted acid catalyzed sol–gel process, the silica structure was formed with a high SiOH content strongly interacting with the epoxy matrix (through H-bonding with a POP based network chain) thus increasing the modulus. Moreover, the IL C_7O_3MImMeS acted as a system compatibilizer in which the IL anion interacted with the OH-groups on the silica surface, while the cation side-chain interacted with the epoxy network chains (Scheme 1b). Due to this compatibilization an enhancement of the silica–epoxy interaction occurs and the modulus further grows. The resulting dynamic interphase interaction undergoes a breaking–formation process under stress, which was responsible for the enhanced ductility of the system.

Combining the reinforcing effect of ILs with the GTMS toughening effect resulted in well-balanced tensile properties. Consequently, by a combination of GTMS and different ILs one can tune and balance the tensile properties of the epoxy-silica nanocomposites to reach the required stiffness and toughness.

The stiff and brittle "C_{10}MImBF_4-HCl nanocomposite" was toughened by GTMS. This hybrid presented a very high elongation at break, but the modulus drop was too pronounced in this case (Fig. 4, curve e30). GTMS modified the network structure and likely caused perturbation and destabilization of the reinforcing IL C_{10}-chain self-assembly. In contrast, Fig. 3 and 4 showed that the IL C_7O_3MImMeS is more suitable in combination with GTMS, providing better balanced tensile properties. This strategy yielded materials with very high toughness, while keeping a considerably high modulus and a very high strength (Table 1, entries 10–12). The best balanced tensile properties were achieved in the nanocomposites prepared using IL C_7O_3MImMeS with an optimum GTMS content of 20–30 mol%. The stress–strain curve d30 in Fig. 4 illustrates stress softening at about 20% elongation, reflecting breakage of silica–epoxy interphase interaction modified with the IL. The silica debonding and plastic yield of the interphase is assumed to be the reason for the strongly enhanced toughness. These nanocomposites displayed a modulus, tensile strength and energy to break higher by ~450%, ~500% and more than one order of magnitude, respectively, compared to the one-step epoxy-silica hybrid (Table 1, entry 2 *vs.* 12). One should keep in mind that the one-step hybrid shows a comparable performance to both epoxy-CB and epoxy-CNF nanocomposites. Comparison to the unmodified epoxy network DGEBA-D2000 is impressive; the optimized hybrid exhibited almost a one order of the magnitude higher modulus and tensile strength, and more than 25 times higher energy to break (Table 1, entry 1 *vs.* 12). One has to take into account the poor properties of the neat network.

In order to gain deeper insight into the tensile behavior of our systems we have performed experiments showing the prestrain-induced softening denoted as the Mullins effect. The Mullins-type stress-softening is assumed to result from a stress-induced nanofiller cluster breakdown[32] or the disruption of matrix–filler bonds.[33] The sample underwent an extension–retraction cycle and after a certain time at rest, to allow a partial system relaxation, the specimen was stretched in the second cycle to a higher strain than in the previous one, and so on. A set of extension–retraction cycles to the strain $\varepsilon = 0.05, 0.10, 0.20, 0.30, 0.40$ was carried out up to rupture of the specimen as shown in Fig. 5 for the nanocomposite prepared in the presence of IL C_7O_3MImMeS and 30 mol% GTMS. The sample prestrained up to a certain strain shows a softening in the next extension. This is a result from the breaking and slipping of the silica–epoxy contacts occurring during the prestrain. It implies that the original silica–epoxy interphase has not been restored during the relaxation at rest. The effect is most pronounced at the highest prestrain, $\varepsilon = 0.40$. The stress–strain curve displays a significant hysteresis in the corresponding extension–retraction cycle as a result of the stress softening and a highly retarded elastic response of the viscoelastic polymer. The hysteresis is attributed to the energy dissipated by the material during deformation. The sample exhibits a plastic permanent deformation (tension set) remaining at the end of the cycle despite a partial relaxation during the interval at rest. This tension set increases in each cycle, reaching 7% after the last prestrain. The Figure shows that small elongations ($\varepsilon = 0.05$ and 0.10) and the respective corresponding stresses ($\sigma \sim 2$ MPa and 3.5–4 MPa) induced very small tension sets (0.2% and 1%, respectively) and no significant hysteresis. Only prestraining of $\varepsilon = 0.20$ and the corresponding stress $\sigma \sim 5$ MPa resulted in a large plastic deformation and hysteresis. Consequently, above the critical stress, at ~4 MPa (under experimental conditions at room temperature and a rate of the strain of 1 mm min^{-1}, *i.e.* ~5% min^{-1}) the interphase contacts broke down and slid giving rise to a pseudo-yield phenomenon and the beginning of the stress softening. The local plastic

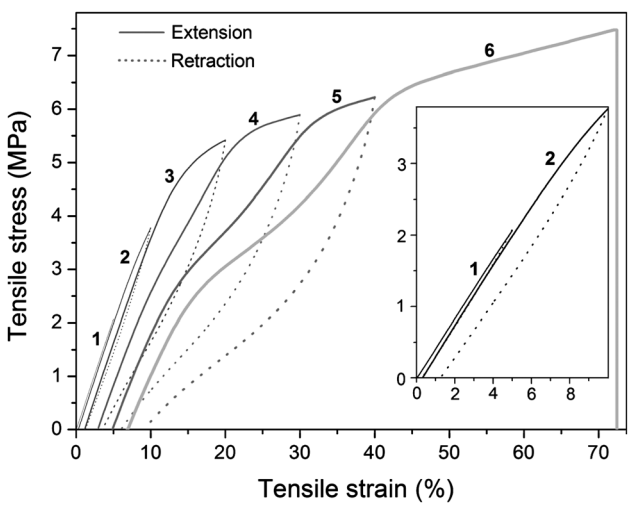

Fig. 5 Mullin-type stress-softening after prestraining of the nanocomposite with IL C_7O_3MImMeS and 30 mol% GTMS. Extension–retraction cycles to ε = (1) 0.05, (2) 0.10, (3) 0.20, (4) 0.30, (5) 0.40; and (6) extension until rupture.

deformation, *i.e.* sliding and disruption of the interphase, leads to an increase in the finite extensibility ε_b.

The IL C_6MImMeS was not studied before as an additive in the preparation of epoxy-silica nanocomposites. Its application produced a hybrid with considerable toughness enhancement and the best balanced tensile properties among the GTMS-free samples. The hybrid showed a pronounced stress softening resulting in high elongation at break and toughness (Fig. 4, curve f). The observed modulus, tensile strength and elongation at break were almost twice as high, while the energy to break was 3–4 times increased when compared to the two-step nanocomposite (Table 1, entry 3 *vs.* 19). In general, the MeS based ILs promote a stronger interfacial interaction than the ILs with the BF_4 anion.[4] Furthermore, the H-bonding strength between the imidazolium cation and the MeS anion is stronger than between the imidazolium cation and the BF_4 anion.[22] The higher strength of these physical coordinations could be responsible for the higher toughness in the final nanocomposite (compared to the IL C_{10}MImBF$_4$ nanocomposite). At the same time, the smaller aliphatic C_6 side chain of this IL suggests the formation of a weaker self-assembly arrangement and, consequently, the stiffness was not as high as obtained with the hybrid containing C_{10}MImBF$_4$.

The silica–epoxy interphase interaction was experimentally determined using dynamic mechanical analysis. Fig. 6a shows the loss factor tanδ (G''/G') as a function of temperature for the neat epoxy network and the epoxy-silica nanocomposites prepared with or without ILs. The main relaxation peak at $T \sim -25$ °C corresponds to the glass transition of the epoxy network. The nanocomposites displayed a decrease in the maximum of the loss factor amplitude, a broadening of the peak towards higher temperatures or even the appearance of a new maximum/shoulder. On the other hand, Table 2 demonstrates that all nanocomposites, with the exception of the "one-step hybrid", showed a slight shift of T_g (maximum of the peak) to a lower temperature. Such nanocomposite behavior results from two competing nanofiller effects in the polymers. (1) The reduction of chain mobility due to the interaction of the chains with rigid nanostructures and (2) the increase in free volume, leading to the loosened molecular packing of the chains due to the presence of nanostructures. These effects can be described by the two-phase model of polymer dynamics in the polymer hybrids.[34,35] One phase of the nanocomposite exhibits faster and the second phase shows slower chain dynamics with respect to the polymer matrix.

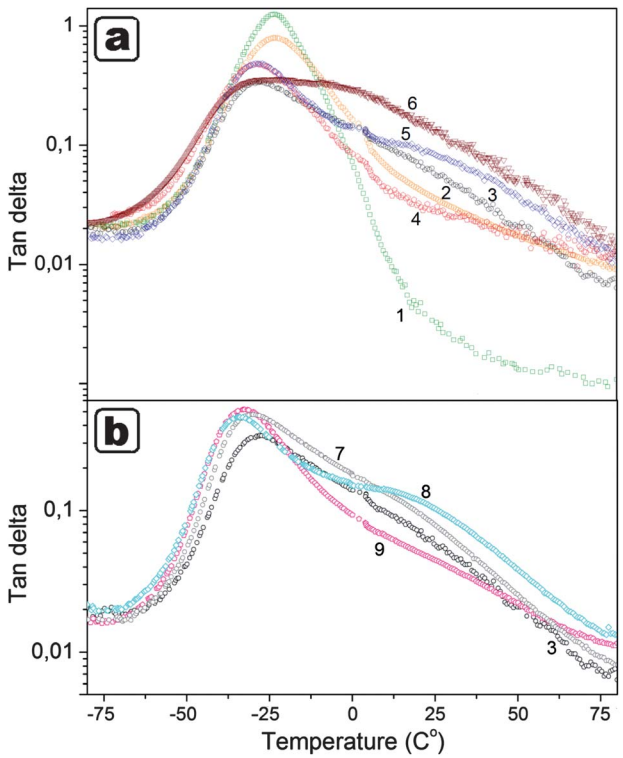

Fig. 6 Loss factor tan δ as a function of temperature for (1) the neat DGEBA-D2000 network; nanocomposites obtained by (2) one-step and (3) two-step processes; with ILs (4) C_{10}MImBF$_4$ + HCl, (5) C_7O_3MImMeS and (6) C_6MImMeS + HCl without GTMS (**a**); also samples (7) two-step process, (8) C_7O_3MImMeS and (9) C_{10}MImBF$_4$ + HCl, all containing 20 mol% GTMS (**b**).

The diminishing of the amplitude of the loss factor corresponds to a reduced content of free unrestricted epoxy chains. The peak broadening characterizes a distribution of chains with reduced mobility and the new peak at higher temperature is assigned to the network chains strongly immobilized by interaction with the silica phase. Fig. 6a proves that while the interaction is quite weak in the case of the one-step hybrid (mild decrease in amplitude with respect to the neat network, narrow peak), the two-step nanocomposite exhibits a strong chain mobility reduction reflected by a loss factor shoulder at $T = 25$ °C.[4] Fig. 6a shows that the nanocomposites formed in the presence of MeS based ILs C_7O_3MImMeS and C_6MImMeS display the lowest amplitude at the maximum tan δ and the most pronounced peak broadening, as well as a shoulder appearing at higher temperature. This is evidence of the effect of these ILs in promoting the silica–epoxy interfacial interaction. The strongest physical dynamic interaction, in the case of C_6MImMeS, is most likely responsible for the high toughness of the corresponding nanocomposite. In contrast, the narrow loss factor peak of the nanocomposite prepared in the presence of IL C_{10}MImBF$_4$ and HCl indicates a much weaker interface interaction leading to a low ductility.

On the contrary, a good dispersion of the silica nanostructures within the network leads to an increase in the free volume and an enhancement of the mobility of a fraction of chains, resulting in

Table 2 T_g values of the epoxy-silica/SSQO nanocomposites

Sample[a]	T_g/°C[b]	Curve[c]	
a	−23	1	
b	−23	2	
c	−27	3	Without GTMS
d	−28	5	
e	−28	4	
c20	−30	7	
d20	−34	8	With GTMS
e20	−33	9	

[a] The same codes as described in Table 1 footnote. [b] Evaluated from maximum tan delta peak, measurement at 1 Hz frequency. [c] Related curves in Fig. 6.

a glass transition temperature decrease. The results in Table 2 indicate that the better silica dispersion and the finer morphology, the larger the shift to lower T_g values. Mainly the system compatibilization and the silica dispersion, by using the coupling agent GTMS and by combination of GTMS with ILs, brings about a pronounced drop of T_g (Fig. 6b). This is in addition to the effect of lower chemical crosslinking density due to the presence of GTMS. The SSQO domains formed from GTMS involve flexible linear siloxane sequences and glycidyloxypropyl substituents. These relatively soft nanostructures reduce the mobility of the epoxy chains to a smaller extent than do the rigid silica domains formed from TEOS in the case of the two-step nanocomposite. This is revealed in Fig. 6b, showing a higher amplitude of the peak maximum and lower loss factor values at high temperatures in the GTMS containing systems. It is obvious that the free volume effect dominates in this case, contributing to an enhancement of toughness at the expense of stiffness.

The best tensile property enhancements were achieved by introducing GTMS and by the application of MeS anion based ILs. In both cases a remarkable homogenization of the nanocomposite morphology was proven due to a strengthening of the interfacial interaction. The resulting hybrids involve small silica/SSQO nanodomains well dispersed in the epoxy matrix. Therefore, we suppose that the toughening effect is a result of a disruption of the interphase rather than a breakdown of small inorganic clusters.

Conclusions

Ionic liquids (ILs) were used to control the morphology and tensile properties of rubbery epoxy-silica nanocomposites. The interphase silica–epoxy interaction was found to be crucial for both nanocomposite morphology and enhanced tensile properties. Homogenization of the organic–inorganic system and improved dispersion of the silica nanodomains in the epoxy matrix were achieved by the two-step simultaneous polymerization procedure and by introducing the coupling agent GTMS in addition to the application of ILs.

Incorporation of GTMS in the epoxy-silica nanocomposite led to an enhancement of the material extensibility and toughness while the strength and modulus decreased due to a lowering of the crosslinking density. In contrast, application of the ILs C_7O_3MImMeS, C_6MImMeS and C_{10}MImBF$_4$ with HCl resulted in a significant stiffening of the system. The strong interphase interactions in the case of the MeS based ILs and physical crosslinking by self-assembly of the C_{10} or C_6 IL side-chains are the reasons for the high nanocomposite moduli. The very high crosslinking density in the case of the C_{10}MImBF$_4$ containing nanocomposite, however, brought about a significant loss of the extensibility and ductility. Better balanced tensile properties were achieved by application of the IL C_6MImMeS, promoting formation of the nanocomposite with a high modulus and tensile strength as well as a high extensibility and toughness.

The materials with the best balanced tensile properties were produced by a combination of ILs and GTMS. The nanocomposite with C_7O_3MImMeS and 20–30% GTMS showed a modulus, tensile strength and energy to break higher by ~450%, ~500% and more than one order of magnitude, respectively, compared to the unmodified one-step epoxy-silica hybrid. The reinforcement of the epoxy elastomer DGEBA-D2000 with silica, GTMS and ILs was found to be much more efficient than the application of carbon black or carbon nanofibers (CNF) described in the literature.[29] The optimal epoxy-silica nanocomposites show 7–8 times higher modulus and 2–3 times higher tensile strength and energy to break compared to the epoxy-CNF system. The enhanced toughness of the modified epoxy-silica nanocomposites is a result of a stress-induced disruption of the strong silica-epoxy interaction and sliding at the interphase layer resulting in a plastic yield.

Altogether, the application of ILs and GTMS enabled the tuning of the tensile properties from stiff quasi-brittle materials in the case of the epoxy-silica hybrid with C_{10}MImBF$_4$ up to the very tough hybrid prepared by using C_7O_3MImMeS in synergy with GTMS. This use of ILs as property tuning additives proved to be a step further for the preparation of advanced materials with a high modulus and a tunable balance between stiffness and toughness.

Acknowledgements

The authors acknowledge the financial support of the Grant Agency of the Czech Republic (P108/12/1459) and the Academy of Sciences of the Czech Republic for support in the frame of the Program of International Cooperation (M200500903). R. K. D. is grateful to the National Council of Scientific and Technological Development (CNPq) of the Brazilian government for the financial support.

Notes and references

1 Y. Zhou, J. H. Schattka and M. Antonietti, *Nano Lett.*, 2004, **4**, 477–481.
2 R. K. Donato, M. V. Migliorini, M. A. Benvegnú, M. P. Stracke, M. A. Gelesky, F. A. Pavan, C. M. L. Schrekker, E. V. Benvenutti, J. Dupont and H. S. Schrekker, *J. Sol-Gel Sci. Technol.*, 2009, **49**, 71–77.
3 M. V. Migliorini, R. K. Donato, M. A. Benvegnú, R. S. Gonçalves and H. S. Schrekker, *J. Sol-Gel Sci. Technol.*, 2008, **48**, 272–276.
4 R. K. Donato, L. Matějka, H. S. Schrekker, J. Pleštil, A. Jigounov, J. Brus and M. Šlouf, *J. Mater. Chem.*, 2011, **21**, 13801–13810.
5 Y. Ye, C. Tseng, W. Shen, J. Wang, K. Chen, M. Cheng, J. Rick, Y. Huang, F. Chang and B. Hwang, *J. Mater. Chem.*, 2011, **21**, 10448–10453.
6 S. Livi, J. Duchet-Rumeau, T. Pham and J. F. Gérard, *J. Colloid Interface Sci.*, 2010, **349**, 424–433.
7 T. Fukushima, A. Kosaka, Y. Yamamoto, T. Aimiya, S. Notazawa, T. Takigawa, T. Inabe and T. Aida, *Small*, 2006, **2**, 554–560.
8 R. Mincheva, F. Meyer, P. Verge, J. Raquez, L. Billiet, F. DuPrez and P. Dubois, *Macromol. Rapid Commun.*, 2011, **32**, 1960–1964.
9 J. Dupont, R. F. de Souza and P. A. Z. Suarez, *Chem. Rev.*, 2002, **102**, 3667–3692.
10 N. H. Kim, S. V. Malhotraand and M. Xanthos, *Microporous Mesoporous Mater.*, 2006, **96**, 29–35.
11 T. Welton, *Chem. Rev.*, 1999, **99**, 2071–2083.
12 J. Dupont and P. A. Z. Suarez, *Phys. Chem. Chem. Phys.*, 2006, **8**, 2441–2452.
13 R. K. Donato, M. V. Migliorini, M. A. Benvegnú, J. Dupont, R. S. Gonçalves and H. S. Schrekker, *J. Solid State Electrochem.*, 2007, **11**, 1481–1487.
14 J. Wen and J. E. Mark, *J. Appl. Polym. Sci.*, 1995, **58**, 1135–1145.
15 L. Bokobza and J. P. Chauvin, *Polymer*, 2005, **46**, 4144–4151.
16 G. Heinrich, M. Klüppel and T. A. Vilgis, *Curr. Opin. Solid State Mater. Sci.*, 2002, **6**, 195–203.
17 A. I. Medalia, *Rubber Chem. Technol.*, 1978, **51**, 437–519.
18 L. Matějka, O. Dukh and J. Kolařík, *Polymer*, 2000, **41**, 1449–1459.

19 L. Mascia, L. Prezzi and B. Haworth, *J. Mater. Sci.*, 2006, **41**, 1145–1155.
20 M. Battistella, M. Cascione, B. Fiedler, M. H. H. Wichmann, M. Quaresimin and K. Schulte, *Composites, Part A*, 2008, **39**, 1851–1858.
21 H. S. Schrekker, D. O. Silva, M. A. Gelesky, M. P. Stracke, C. M. L. Schrekker, R. S. Gonçalves and J. Dupont, *J. Braz. Chem. Soc.*, 2008, **19**, 426–433.
22 C. C. Cassol, G. Ebeling, B. Ferrera and J. Dupont, *Adv. Synth. Catal.*, 2006, **348**, 243–248.
23 L. Matějka, J. Pleštil and K. Dušek, *J. Non-Cryst. Solids*, 1998, **226**, 114–121.
24 L. Matějka, K. Dušek, J. Pleštil, J. Kříž and F. Lednický, *Polymer*, 1999, **40**, 171–181.
25 L. Matějka, in *Hybrid Nanocomposites for Nanotechnology*, Springer Verlag, New York, 2009, p. 3–85.
26 L. Matějka, O. Dukh, J. Brus, W. J. Simonsick and B. Meissner, *J. Non-Cryst. Solids*, 2000, **270**, 34–47.
27 L. Matějka, O. Dukh, D. Hlavatá, B. Meissner and J. Brus, *Macromolecules*, 2001, **34**, 6904–6914.
28 L. Matějka, O. Dukh, B. Meissner, D. Hlavatá, J. Brus and A. Strachota, *Macromolecules*, 2003, **36**, 7977–7985.
29 P. Richard, T. Prasse, J. Y. Cavaille, L. Chazeau, C. Gautier and J. Duchet, *Mater. Sci. Eng.*, 2003, **A352**, 344–348.
30 L. Matějka, O. Dukh, H. Kamišová, D. Hlavatá, M. Špírková and J. Brus, *Polymer*, 2004, **45**, 3267–3276.
31 J. Macan, H. Ivankovic, M. Ivankovic and H. J. Mencer, *J. Appl. Polym. Sci.*, 2004, **92**, 498–505.
32 M. Klüppel and J. A. Schramm, *Macromol. Theory Simul.*, 2000, **9**, 742–754.
33 S. Göktepe and C. J. Miehe, *J. Mech. Phys. Solids*, 2005, **53**, 271–281.
34 A. Sargsyan, A. Tonoyan, S. Davtyan and C. Schick, *Eur. Polym. J.*, 2007, **43**, 3113–3127.
35 T. Kourkoutsaki, E. Logakis, I. Kroutilová, L. Matějka, J. Nedbal and P. Pissis, *J. Appl. Polym. Sci.*, 2009, **113**, 2569–2582.